1 **Cr(VI) Effect on Tc-99 Removal from Hanford Low-Activity Waste Simulant by Ferrous**

2 **Hydroxide**

3

4 Sarah A. Saslow[1], Wooyong Um[1,*], Carolyn I. Pearce[1], Mark E. Bowden[2], Mark H. Engelhard[2],

5 Wayne L. Lukens[3], Dong-Sang Kim [1], Michael J. Schweiger [1], and Albert A. Kruger [4]

6

7 [1]*Pacific Northwest National Laboratory, 902 Battelle Blvd, Richland, WA, 99352, USA*

8 [2]*Environmental Molecular Sciences Laboratory, Pacific Northwest National Laboratory,*

9 *Richland, WA, 99354, USA*

10 [3]*Lawrence Berkeley National Laboratory, 1 Cyclotron Rd, Berkeley, CA, 94720 USA*

11 [4]*United States Department of Energy, Office of River Protection, P.O. Box 450, Richland, WA*

12 *99352, United States*

13 *Corresponding author: Wooyong Um, Pacific Northwest National Laboratory, 902 Battelle

14 Blvd., PO Box 999, P7-54, Richland, WA 99352, USA. Telephone: (509)-371-7175. Fax: (509)-

15 371-7344. Email address: wooyong.um@pnnl.gov. Now at Pohang University of Science and

16 Technology (POSTECH); Email address: wooyongum@postech.ac.kr

17

18 **Abstract**

19   Here, Cr(VI) effects on Tc-immobilization by $Fe(OH)_2(s)$ are investigated while assessing

20 $Fe(OH)_2(s)$ as a potential treatment method for Hanford low-activity waste destined for

21 vitrification. Batch studies using simulated low-activity waste indicate that Tc(VII) and Cr(VI)

22 removal is contingent on reduction to Tc(IV) and Cr(III). Furthermore, complete removal of both

23 Cr and Tc depends on the amount of $Fe(OH)_2(s)$ present, where complete Cr and Tc removal

24 requires more $Fe(OH)_2(s)$ (~200 g/L of simulant), than removing Cr alone (~50 g/L of simulant).

25   XRD analysis suggests that $Fe(OH)_2(s)$ reaction and transformation in the simulant produces

26   mostly goethite (α-FeOOH), where $Fe(OH)_2(s)$ transformation to goethite rather than magnetite

27   is likely due to the simulant chemistry, which includes high levels of nitrite and other

28   constituents. Once reduced, a fraction of Cr(III) and Tc(IV) substitute for octahedral Fe(III)

29   within the goethite crystal lattice as supported by XPS, XANES, and/or EXAFS results. The

30   remaining Cr(III) forms oxide and/or hydroxide phases, whereas Tc(IV) not fully incorporated

31   into goethite persists as either adsorbed or partially incorporated Tc(IV)-oxide species. As such,

32   to fully incorporate Tc(IV) into the goethite crystal structure, additional $Fe(OH)_2(s)$ (>200 g/L of

33   simulant) may be required.

34

35   **TOC**

36
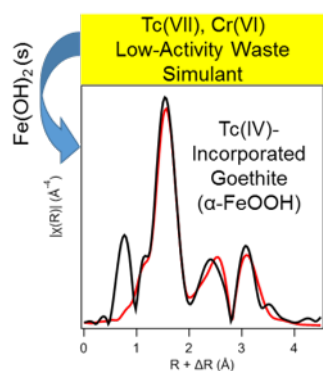
1. Introduction

Technetium-99 (Tc) is a radioactive fission product present at nuclear waste legacy sites that is problematic due to its long half-life (2.1×10^5 years), high fission yield (~6%), and environmental mobility as Tc(VII) species in oxidizing environments.[1-3] Unfortunately, nuclear waste treatment and environmental remediation strategies targeting Tc are hindered by current high temperature treatment technologies and the presence of co-mingled redox-active competitors, e.g. Cr(VI). [4-5] For example, at the US Department of Energy Hanford Site (Washington State, USA) the baseline treatment plan for nuclear waste is vitrification,[6-7] which requires operating temperatures >1000 °C that consequently causes Tc volatilization and low Tc-retention in the glass waste form. One strategy to overcome Tc volatilization is reduction of Tc(VII) to stable Tc(IV) with concurrent Tc(IV) incorporation into minerals,[7-14] although this treatment method is often complicated by the presence of co-mingled Cr(VI), which was used as a corrosion inhibitor in Hanford nuclear waste storage tanks.[4] Cr(VI) has a more favorable reduction potential, -0.16 V vs -0.36 V for Tc(VII) at pH 14,[15-16] and exists in Hanford nuclear waste streams at concentrations orders of magnitude greater than Tc.[17] As a result, reductants added to reduce Tc(VII) are consumed by Cr(VI). Thus, there remains a critical need for treatment technologies that can reduce Tc(VII) in the presence of Cr(VI).

In a preliminary study, ferrous hydroxide solid ($Fe(OH)_2(s)$) was successfully used to reduce Tc(VII) in the presence of Cr(VI) and incorporate Tc(IV) into magnetite via $Fe(OH)_2(s)$ mineral transformation under oxic conditions.[18] This work was performed under the high ionic strength and pH conditions expected for Hanford low-activity waste (LAW) streams, but used a simple solution chemistry that only considered Tc(VII) and Cr(VI) in 1 M NaOH. Here, $Fe(OH)_2(s)$ is used to treat Tc in a simulated LAW solution, to assess (i) how complex and realistic waste

60 streams affect the efficacy of this approach and (ii) provide mechanistic evidence for Cr(VI)

61 reduction and solid formation and how this impacts the $Fe(OH)_2(s)$ treatment mechanism for Tc.

62 Hanford's liquid radioactive/chemical waste, currently stored in tanks but destined for pre-

63 treatment and vitrification, varies from tank to tank due to the different separation processes used

64 for spent nuclear fuel, resulting in complex mixtures of nitrate, nitrite, phosphate, sulfate, and

65 organic based solvents.[19] As such, the exact LAW composition for treatment is not known, so for

66 the purpose of this work, an overall average LAW simulant composition is used based on output

67 from the Hanford Tank Waste Operations Simulator (HTWOS) model.[17] To arrive at this average

68 composition, which includes nitrate, nitrite, sulfate, aluminum, Cr(VI) and other minor

69 constituents, the HTWOS model tracks tank waste storage, retrieval, and multiple treatment and

70 immobilization processes over ~20 years of operation.

71 The treatment approach described here involves reduction of Tc(VII) in the presence of

72 Cr(VI) and removal of Tc from solution through incorporation into a solid iron oxide/hydroxide

73 phase. Once reduced and stabilized, Tc is expected to be resistant to release from the iron

74 oxide/hydroxide product(s), which may stabilize Tc during vitrification and increase Tc loading

75 into glass. In addition, development and implementation of this approach could improve

76 environmental remediation efforts that target co-mingled Tc(VII) and Cr(VI) contaminated

77 areas.[21]

78 **2. Experimental**

79 **$Fe(OH)_2(s)$ Synthesis.** A detailed synthesis procedure for $Fe(OH)_2(s)$ and product

80 characterization may be found in previously published work.[18] Briefly, $Fe(OH)_2(s)$ was prepared

81 and stored inside an anoxic chamber (Coy Laboratories) that was maintained using a gas mix of

82 N_2 (98%) and H_2 (2%). $Fe(II)Cl_2·4H_2O$ (14 g, >95%, Fisher Scientific) was dissolved in N_2-

100 purged double deionized water (400 g, DDI, Millipore 18Ω). Dissolved Fe(II) was then

101 precipitated as $Fe(OH)_2$(s) by adding 8.2 mL of 10 M NaOH (Fisher Scientific) to solution and

102 mixing by hand. The solid was allowed to react overnight and then separated from the

103 supernatant using a 0.45 µm Nalgene® filter. The $Fe(OH)_2$(s) was then allowed to dry for 24

104 hours before it was powdered using a mortar and pestle.

105   **Simulant Preparation.** A 5 M Na Hanford LAW simulant with 1080 ppm Cr(VI) was

106 generated as described previously,[17] and spiked with 1-100 ppm Tc(VII), using a 10,000 mg/L

107 Tc stock solution (NH_4TcO_4). The starting simulant was characterized using ion chromatography

108 (IC) and inductively coupled plasma optical emission spectrometry (ICP-OES) (Table 1).

109 **Table 1.** 5 M Na Average LAW Simulant Composition

Constituent	Target Concentration [mg/L]*	Measured Concentration [mg/L]	Constituent	Target Concentration [mg/L]*	Measured Concentration [mg/L]
Al	8280	8500	F^-	600	<1000
Cr	1120	1080	Cl^-	1500	<2500
P	1520	981	NO_2^-	26,000	26,800
K	1280	1300	Br^-	-	<5000
Na	115,000	110,000	NO_3^-	101,000	102,000
S	2740	2810	SO_4^-	-	10,100
Ti	-	7.84	PO_4^-	-	<7500
pH		13.5	E_h (SHE)		26 – 81 mV

* Target Concentrations from Russell et al, 2013 for 5 M Na Average LAW Simulant;[17] target and measured concentrations determined using IC and ICP-OES.
-: Not identified
(SHE): Standard Hydrogen Electrode corrected

110

111   **Tc(VII) and Cr(VI) Treatment by $Fe(OH)_2$(s).** $Fe(OH)_2$(s) (~0.1-1.2 g) was added to LAW

112 simulant to achieve final $Fe(OH)_2$(s):simulant ratios between 1 and 360 g/L. $Fe(OH)_2$(s) was

113 removed from the anaerobic chamber immediately before simulant addition, after which

114 sample(s) reacted for 3 days (± 1 hour) in an oven set to 75 °C with occasional hand mixing. In

115 some instances, aliquots of $Fe(OH)_2$(s) were added sequentially over the reaction period.[18] For

116 these samples, each aliquot of $Fe(OH)_2$(s) was allowed to react with the simulant for ~24 hours

118   before sampling and subsequent Fe(OH)$_2$(s) addition. After 3 days, all samples were allowed to

119   cool for $\geq$ 2 hours before the solid product was separated from the supernatant (0.45 μm

120   Nalgene® filter), rinsed with ~50 mL of DDI, and air-dried for $\geq$ 24 hours. The supernatant was

121   analyzed to determine final Cr (ICP-OES) and Tc (ICP-MS) concentrations. The final pH of a

122   representative set of supernatants was 13.5 $\pm$ 0.1 and the E_h (SHE) ranged from 26 to 81 mV

123   before and after the 3 day reaction period.

124   **X-ray Photoelectron Spectroscopy (XPS).** Samples were prepared by dusting carbon tape

125   with dry sample powder. Tc-free samples were analyzed using a Physical Electronics Quantera

126   Scanning X-ray Microprobe equipped with a focused monochromatic Al Kα X-ray (1486.7 eV)

127   source for excitation and a spherical section analyzer. Tc-containing samples were analyzed

128   using a Kratos Axis DLD spectrometer with a monochromatic Al Kα X-ray source. An 80 W X-

129   ray beam was focused to 100 μm (diameter) and scanned over the sample. High-energy

130   resolution spectra were collected using a pass-energy of 69.0 eV and 0.125 eV step size. Spectra

131   were charge-corrected to the main line, carbon 1s peak at 285.0 eV. Data analysis and peak

132   fitting was performed in CasaXPS (version 2.3.15) (see SI for details).

133   **X-ray Diffraction (XRD).** XRD patterns were collected using a Rigaku Miniflex II XRD

134   unit equipped with a Cu Kα radiation (λ=1.5418 Å, 30-40 kV, 15 mA) source. Samples were

135   scanned, at minimum, between 3 − 90 degrees 2θ at 0.5 degrees/min using a 0.02 degree step

136   size. Reitveld quantification refinements were performed for each pattern collected (see SI for

137   details).

138   **X-ray Absorption Near Edge Structure (XANES) and Extended X-ray Absorption Fine**

139   **Structure (EXAFS) Spectroscopy.** Tc K-edge (21,044 eV) spectra were collected on beamline

140   11-2 at the Stanford Synchrotron Radiation Laboratory (SSRL) for samples spiked with Tc

141   concentrations $\geq$100 mg/L. Cr K-edge (5,989 eV) spectra were collected on SSRL beamlines 11-

142   2 and 4-1. Dead-time correction and data reduction was performed using SixPack.[22] Data

143   analysis was performed using ATHENA/ARTEMIS software.[23] Tc XANES spectra were energy

144   calibrated using a Tc(VII) reference (pertechnetate (TcO_4^-) adsorbed on Reillex-HPQ polymer

145   resin) and fit using a linear combination of Tc(IV) and Tc(VII) standards.[14, 24-25] For EXAFS

146   fitting, a Tc-substituted goethite (α-FeOOH) structure was used in addition to models for

147   $TcO_2 \cdot 2H_2O$ and TcO_4^- as necessary. Cr XANES spectra were energy calibrated using a Cr foil

148   reference and fit using a linear combination of Cr(III) and Cr(VI) standards. Additional sample

149   preparation and analysis details are provided in the SI.

150

151   **3. Results and Discussion**

152   **Tc(VII) and Cr(VI) Removal by Fe(OH)₂(s).** A viable material for removing contaminants

153   from LAW must stabilize Tc with as little solid as possible to meet glass composition constraints

154   and avoid costly operational changes. The minimum $Fe(OH)_2$(s) required to remove co-mingled

155   Tc and Cr from the LAW simulant was determined as a function of $Fe(OH)_2$(s):simulant ratio

156   (Figure 1). Studies performed without Tc indicate that 50 g of $Fe(OH)_2$(s) per liter of simulant is

157   required to remove Cr (1080 ppm) from solution. The addition of 1 ppm Tc does not change the

158   minimum $Fe(OH)_2$(s) required to remove Cr(VI); though to remove >97.6% Tc requires at least

159   200 g $Fe(OH)_2$(s) per liter of simulant.
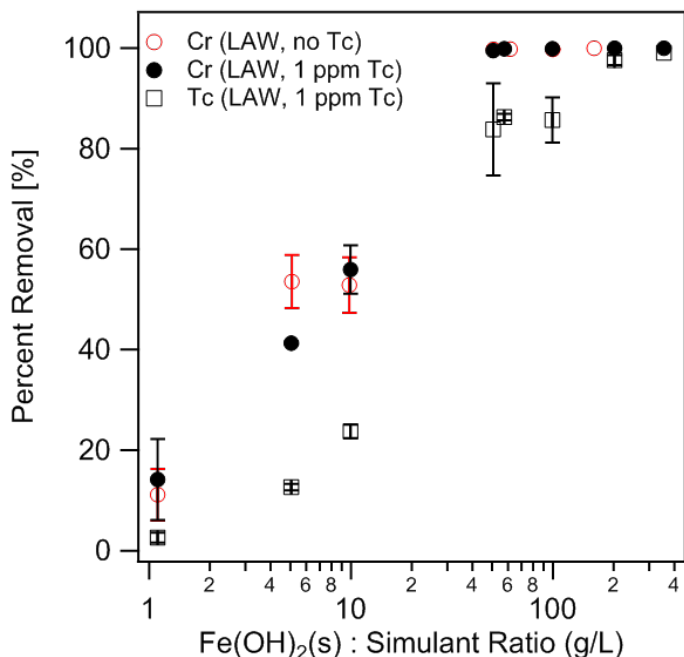
Figure 1. Cr and Tc removal from LAW simulant with 1 ppm Tc (black) and without Tc (red). Cr(VI) results are indicated by filled or open circles, Tc results by open squares. Error bars represent the standard deviation of results averaged from two to six replicate samples. Percent removal assumed to be 100% if below ICP-OES detection limit for Cr (23 µg/L) or ICP-MS detection limit for Tc (33 ng/L).

To better understand the additional $Fe(OH)_2(s)$ requirement needed to remove Tc(VII) from the LAW simulant, the solution chemistry and redox and transformation processes must be considered. Similar to the 1 M NaOH system,[18] the experimentally determined amount of $Fe(OH)_2(s)$ needed to remove Tc (1 ppm) and Cr (1080 ppm) is ~35x more than the amount needed to reduce Tc(VII) to Tc(IV), and Cr(VI) to Cr(III), based solely on redox requirements. This is partially attributed to rapid oxidation of Fe(II) to Fe(III) by air and the additional Fe(II) needed to form iron oxide/hydroxide phases that incorporate Tc and/or Cr,[10, 26-29] but is likely also the result of the complex chemical environment, e.g., pH and competing contaminants in the LAW simulant that require excess reductant due to competing chemical processes. For instance, the Tc and Cr Pourbaix diagrams (see SI) for the simulant solution (Table 1), assuming 200 g of $Fe(OH)_2(s)$ per liter, suggest that both constituents should remain in solution as oxidized TcO_4^-

177 and CrO_4^{2-} given the pH and E_h conditions measured before $Fe(OH)_2(s)$ addition and after the 3

178 day reaction period. The Pourbaix diagrams predict that Fe(II) would preferentially facilitate the

179 reduction and volatilization of nitrate and nitrite as $N_2(g)$, with the remaining Fe(II) precipitating

180 as the spinel hercynite $(Fe(II)Al(III)_2O_4)$.[30-31] Yet, at a 200 g/L $Fe(OH)_2(s)$:simulant ratio, neither

181 Tc nor Cr are detected in solution at significant concentrations. Additionally, IC measurements

182 of the remaining solution indicate negligible removal of nitrate and only ~45% removal of

183 nitrite. Al(III) removal was determined to increase by ~45% with increasing $Fe(OH)_2(s)$:simulant

184 ratio as determined by ICP-OES analysis, but was not completely removed as thermodynamics

185 would predict in the Pourbaix diagrams. In the absence of *in situ* E_h measurements during

186 reaction, these measurements demonstrate that the reduction potential of the simulant solution

187 was significantly lowered upon addition of $Fe(OH)_2(s)$. Furthermore, kinetic processes may

188 overcome thermodynamics early in the reaction, and as a result of these competing processes Tc

189 and Cr are removed from solution.

190 Additional evidence for both a thermodynamically- and kinetically-driven system is that Tc

191 removal is not contingent on complete Cr(VI) removal from the LAW simulant. Both

192 contaminants are removed concurrently, despite a more favorable reduction potential for Cr(VI)

193 versus Tc(VII).[32] This behavior is evident in Figure 1, where, between $Fe(OH)_2(s)$:simulant ratios

194 5-50 g/L, Tc removal begins before Cr removal has reached ~100%. However, between 50-100

195 g/L, Tc removal plateaus until the $Fe(OH)_2(s)$:simulant ratio reaches 200 g/L. This was not seen

196 in the simplified system and could be attributed to the presence of nitrite, which may compete

197 more aggressively for reducing electrons without Cr(VI) present.

198 Finally, based on conclusions derived previously, the removal of Cr(VI) by $Fe(OH)_2(s)$ in the

199 LAW simulant should be contingent on Cr(VI) reduction to Cr(III).[18] Using the IC/ICP-MS

201 method previously reported[30] and detailed in the SI, the speciation of Cr in the final supernatant

202 was determined using stable mass isotope ^{52}Cr. Duplicate experiments with a

203 $Fe(OH)_2(s)$:simulant ratio of 9.8 g/L, a ratio below the requirement for complete Cr(VI) removal,

204 removed only 53(6) % of Cr from the LAW simulant with the rest remaining as Cr(VI) in

205 solution. This alludes to a reduction requirement for Cr(VI) removal that is confirmed via solid

206 characterization in the following sections. Removal of Tc(VII) from solution is also expected to

207 occur via reduction to Tc(IV).

208 **Tc and Cr Immobilization in the Solid Phase**

209 *Solid Characterization by XRD:* Solid phase(s) identification is critical for drawing mechanistic

210 conclusions from Cr and Tc immobilization. Two Tc-free samples prepared at 50 and 100 g/L

211 $Fe(OH)_2$:simulant ratios were analyzed by XRD to identify and quantify the minerals formed

212 (Table 2, XRD patterns in the SI). For both samples, goethite (α-FeOOH) accounts for 77% –

213 81% of the solid despite doubling the $Fe(OH)_2(s)$:simulant ratio. The remaining solid is

214 comprised of feroxyhyte (δ-FeOOH), 14 – 17%, and trace amounts (1 – 6%) of amorphous

215 material and/or hematite (Fe_2O_3). High resolution Fe XPS scans collected from three samples

216 with $Fe(OH)_2(s)$:simulant ratios ranging from 50-200 g/L corroborate these XRD results, where

217 83-89 atomic % of Fe is present as goethite (Table 2).

218 **Table 2.** XRD and High Resolution XPS Analysis of Select Solid Phases

Sample		LAW-50-0Tc-1	LAW-100-0Tc	LAW-200-100Tc
$Fe(OH)_2(s)$:Simulant Ratio	g/L	50	100	200
Starting [Tc(VII)]	ppm	0	0	100
XRD Analysis				
Goethite (α-FeOOH)	wt%	77	81	-
a	(Å)*	4.602(2)	4.597(3)	-
b	(Å)*	9.920(3)	9.913(2)	-
c	(Å)*	3.0096(9)	3.0080(9)	-
Crystal Size	(nm)**	9.8(1)	10.7(1)	-
Feroxyhyte (δ-FeOOH)	wt%	17	14	-
Hematite (Fe_2O_3)	wt%	-	3	-
Amorphous/Unidentified	wt%	6	1	-

Survey XPS Analysis[**]				
Cr 2p	at %[*]	1.6(1)	1.1(1)	0.13(1)
Tc 3d	at %	-	-	0.14(3)
Fe 2p	at %	7.3(4)	8.4(8)	1.7(2)
C 1s	at %	27(4)	19(6)	24(1)
O 1s	at %	64(3)	71(5)	74(1)
Cr XPS Analysis[**]				
CrOOH	at %	46(1)	38(14)	59(2)
Cr_2O_3	at %	28(10)	43(19)	32(4)
$Cr(OH)_3$	at %	24.7(2)	18(5)	1(2)
Cr(VI)	at %	1.5	1.3(5)	8.3(8)
Tc XPS Analysis[**]				
Tc(VII)	at %	-	-	52(1)
Tc(IV)	at %	-	-	48(1)
Fe XPS Analysis[**]				
$FeCr_2O_4$	at %	0	0	5.7(2)
Fe_3O_4	at %	12(1)	11(2)	11(1)
FeOOH	at %	88(1)	89(2)	83(1)

(-) No Detected or Analyzed (*) Atomic percent

Goethite (α-FeOOH)[33]: a = 4.634 Å, b = 9.945 Å, c = 3.0321 Å

[*]Values in parentheses are ±3σ, based on the error associated with the Reitveld refinement.

[**] Values in parentheses are ±1σ. For XPS, the standard deviation is determined from of the average of two replicate spot analyses collected for each sample.

219

220   The formation of goethite instead of magnetite,[18, 34-35] or hercynite (as predicted by

221   Pourbaix diagrams presented in the SI), suggests that the solid product is also heavily influenced

222   by co-mingled constituents. As previously mentioned, an $Fe(OH)_2$(s):simulant ratio of ~200 g/L

223   removes ~45% (~12,200 mg/L) of the simulant nitrite and ~45% of Al(III) (SI Figure S1). As

224   nitrite reduction continues, the ratio of Fe(III) to Fe(II) increases, as does the OH/Fe ratio, both

225   of which favor the formation of goethite over magnetite.[36] As goethite forms and Tc(VII) is

226   reduced to Tc(IV), incorporation of Tc(IV) into the goethite structure likely occurs via

227   substitution for Fe(III) due to their identical, six coordinate crystal radii (0.785 Å).[27, 37-38]

228   Substitution of Tc(IV) is not expected to significantly influence the bulk mineral phase

229   distribution determined by XRD nor change the goethite lattice parameters. Although charge

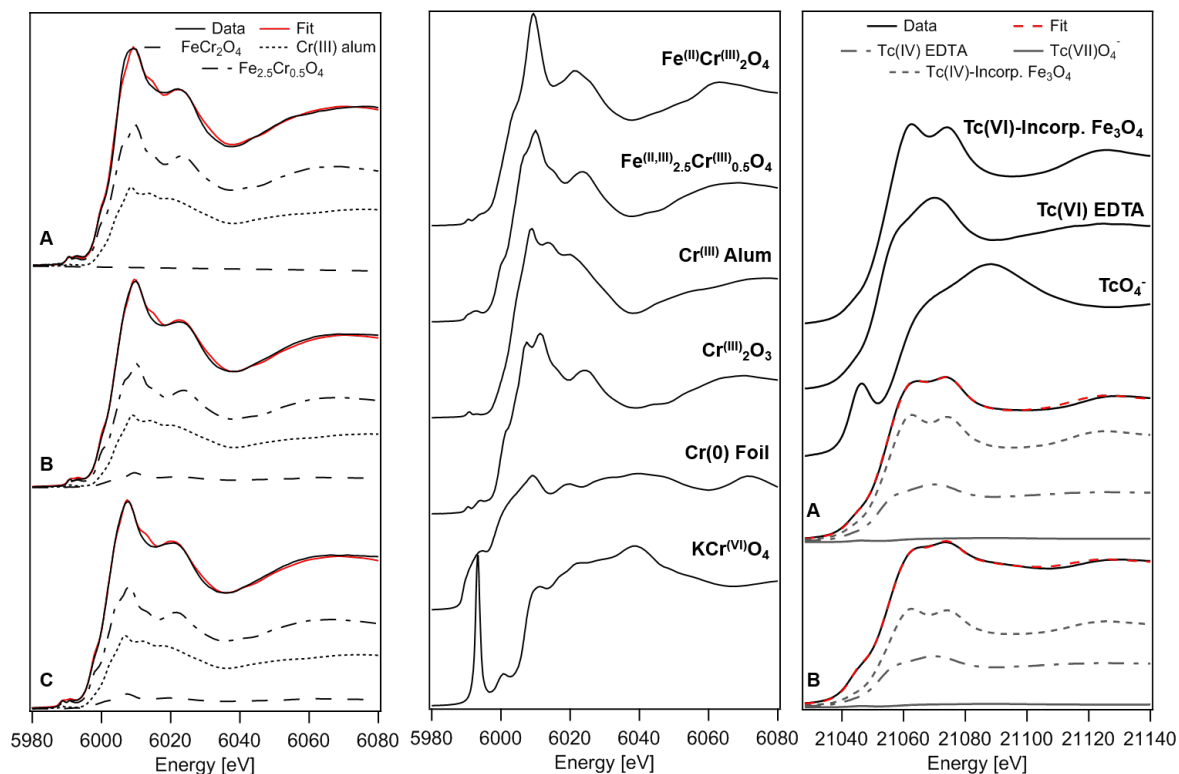230   balance via Fe(II) substitution for Fe(III) may expand the lattice at concentrations higher than

231   those tested here.[10]

232   In contrast, Cr(III) and/or Al(III) substitution into goethite would cause a decrease in

233   calculated goethite lattice parameters since the crystal radius of six coordinate Cr(III), 0.755 Å,

234   and Al(III), 0.670 Å, are smaller than Fe(III).[33, 38-42] Reitveld analysis of collected XRD patterns

235   (Table 2**Error! Reference source not found.**) provides the unit cell parameters a, b, and c for

236   goethite in the absence of Tc. All parameters decrease relative to unsubstituted goethite with

237   increasing $Fe(OH)_2(s)$:simulant ratio.[33] This trend is indicative of increased substitution for

238   Fe(III) by Cr(III) and/or Al(III) in goethite as both constituents are removed from the simulant

239   (Figure 1 and SI Figure S1).

240   *Bulk Solid Phase Cr Speciation Determined by XANES:* Three samples were analyzed by

241   XANES at SSRL to determine the bulk oxidation state and speciation of Cr following reduction

242   and removal by $Fe(OH)_2(s)$ (Figure 2, left panel). As a control, one of the analyzed samples

243   (LAW-50-0Tc) was prepared without Tc and at the minimum $Fe(OH)_2(s)$:simulant ratio needed

244   to remove Cr(VI) from solution, 50 g/L. The remaining two samples were prepared with 100

245   ppm Tc(VII) at two different $Fe(OH)_2(s)$:simulant ratios: 50 g/L (LAW-50-100Tc) and 200 g/L

246   (LAW-200-100Tc). Linear combination analysis (LCA) of each sample initially considered six

247   possible Cr standards: Cr foil, Cr_2O_3, Cr alum ($KCr(SO_4)_2 \bullet 12H_2O$, Cr(III) octahedrally

248   coordinated by water), $Fe_{2.5}Cr_{0.5}O_4$, $FeCr_2O_4$, and K_2CrO_4 (Figure 2, middle panel). It is

249   important to note that Cr(III) forms octahedrally coordinated species both in ordered (iron-

250   containing oxides) and disordered environments. According to XRD results (Table 2), Cr would

251   be incorporated into goethite, not spinel phases such as chromite ($FeCr_2O_4$) or $Fe_{2.5}Cr_{0.5}O_4$.

252   However, without a Cr-substituted goethite standard, $Fe_{2.5}Cr_{0.5}O_4$ and $FeCr_2O_4$ standards are

253   used here to represent the ordered octahedral environment expected for Cr-substituted goethite.[43]

254   Furthermore, the disordered octahedral symmetry of Cr(III) in Cr alum[44] is assumed to represent

255   Cr(III) that has formed separate from the iron phase, e.g., $Cr(OH)_3$ or an amorphous phase with a

256   similar local structure.[45] Standards that did not contribute significantly to the LCA fit (value <

257   2σ) were removed and the data refit using the remaining standards. The final Cr LCA results are

258   shown in Table 3.

259   For all samples, the absence of the prominent Cr(VI) pre-edge feature confirms that Cr is

260   present as Cr(III) and supports the proposed solution removal mechanism that requires Cr(VI)

261   reduction to Cr(III). Furthermore, all samples contained Cr alum (35 – 38 %) and $Fe_{2.5}Cr_{0.5}O_4$

262   (58 – 62 %) as the major phases present regardless of $Fe(OH)_2$:simulant ratio, although for the

263   two samples with a $Fe(OH)_2(s)$:simulant ratio of 50 g/L a small contribution of $FeCr_2O_4$ (6 %)

264   was also determined. Overall, given the low solubility of Cr(III)-containing solids, Cr present in

265   these samples is less susceptible to re-oxidation and release into the environment and exhibits a

266   similar removal mechanism despite changes in Fe(II) resources and Tc(VII) presence.

267

Figure 2. (Left) Normalized and off-set Cr K edge XANES spectra with corresponding LCA fits for Fe(OH)$_2$(s):Simulant ratios (A) 200 g/L, 100 ppm Tc(VII), (B) 50 g/L, 100 ppm Tc(VII), and (C) 50 g/L, no Tc(VII). The LCA fit (red) to the data (black) is the sum of the standard contributions from FeCr$_2$O$_4$ (dash line), Fe$_{2.5}$Cr$_{0.5}$O$_4$ (dot/dash line), and Cr alum (dotted line) determined in the final fit. (Middle) Cr standards considered during LCA fitting, off-set for clarity. (Right) Normalized and off-set Tc K-edge XANES spectra (black) for samples A and B from left panel and the final Tc standards used during LCA fitting. The Tc LCA fit (red dashed line) is the sum of the standard contributions from TcO$_4^-$ (line), TcEDTA (dot/dash), and Tc-incorporated Fe$_3$O$_4$ (dash).

Table 3. LCA and EXAFS Results from Cr and Tc K Edge XANES and EXAFS Spectra

Sample		LAW-50-0Tc	LAW-50-100Tc	LAW-200-100Tc
Fe(OH)$_2$(s):Simulant Ratio	g/L	50	50	200
Starting [Tc(VII)]	ppm	0	100	100
Cr XANES LCA Analysis				
Cr Alum (KCr(SO$_4$)$_2$•12H$_2$O)	%	35(1)	35(1)	38(4)
	p*	<0.001	<0.001	<0.001
Fe$_{2.5}$Cr$_{0.5}$O$_4$	%	58(2)	59(2)	62(4)
	p	<0.001	<0.001	<0.001
FeCr$_2$O$_4$	%	6(1)	6(1)	-
	p	0.287	0.304	-
Tc XANES LCA Analysis				
TcO$_4^-$	%	-	27.2(2)	9.0(3)
	p	-	<0.001	<0.001

Tc(IV) Incorporated Fe$_3$O$_4$	%	-	49(1)	63(1)
	p	-	<0.001	<0.001
Tc(IV) EDTA	%	-	26(1)	30(1)
	p	-	<0.001	<0.001
Tc EXAFS Analysis				
TcO$_4^-$	%	-	33(6)	0(0)
TcO$_2$·2H$_2$O	%	-	32(8)	67(6)
Goethite	%	-	35(3)	33(6)

Values in parenthesis indicate the standard deviation of the last significant figure.

(-) No Detected

(*) Probability that the improvement to the fit by adding the scattering shell is due to random error. A p value < 0.05 indicates that the improvement is greater than 2σ of the fit.

279

280 *Cr Speciation of the Solid Surface Determined by XPS:* Cr speciation was also analyzed by XPS

281 for select solid samples. XPS analysis is specific to the top 5 – 10 nm of the sample surface;

282 however, surface specificity may be limited here due to the small goethite crystal size (~10 nm)

283 determined by Reitveld refinements (Table 2**Error! Reference source not found.**). Narrow,

284 high resolution scans for Cr are shown in Figure S2 for three Cr-containing solid samples with

285 Fe(OH)$_2$(s):simulant ratios of 50, 100, and 200 g/L, where the 200 g/L sample was prepared with

286 100 ppm of Tc(VII). Peak fitting was performed only for the Cr 2p3/2 peak. A single fitting

287 peak was used to account for surface Cr(VI), with three species considered for Cr(III): Cr$_2$O$_3$,

288 CrOOH, and Cr(OH)$_3$. Chromite, FeCr$_2$O$_4$, was initially considered, but did not significantly

289 contribute to any of the sample fits as expected based on XRD and XANES results. CrOOH

290 accounts for Cr(III) oxyhydroxides and/or partial incorporation into goethite. A summary of the

291 Cr-phase distribution is provided in Table 2.

292   From XPS survey scans it is apparent that Cr only accounts for 0.13-1.6 atomic % of the

293 analyzed area, with Cr increasing with decreasing Fe(OH)$_2$(s):simulant ratio. A minor amount of

294 Cr(VI), presumably loosely adsorbed to the sample, was detected in all samples (1.3 – 8.3 atomic

295 %). Cr(OH)$_3$ was the least abundant Cr(III) species detected, decreasing from 24.7(2) atomic %

296 to 1(2) atomic % with increasing Fe(OH)$_2$(s):simulant ratio. However, distribution between the

297   two most abundant Cr(III) species, CrOOH and Cr_2O_3, did not indicate preferential formation of

298   one species over the other as a function of $Fe(OH)_2(s)$:simulant ratio. Although, within error,

299   CrOOH arguably dominates, accounting for ≤59 atomic % of surface Cr (LAW-200-100Tc).

300   This corroborates conclusions derived from XANES analysis and suggests that Cr substitution

301   into goethite is the favored mechanism for immobilization.

302   *Tc Speciation Determined by XANES and XPS:* The oxidation state of Tc immobilized in the

303   solid was determined by LCA of collected Tc K-edge XANES spectra. The Tc K-edge spectra

304   for LAW-200-100Tc and LAW-50-100Tc ($Fe(OH)_2(s)$:simulant ratios 200 g/L and 50 g/L,

305   respectively, each with 100 ppm of Tc(VII)) and the standards used for LCA are provided in

306   Figure 2 (right panel). Initially, LCA considered five Tc standards: TcO_4^-, TcEDTA,[24]

307   $TcO_2 \cdot xH_2O$,[24] Tc-incorporated Fe_3O_4 (magnetite),[12] and Tc(V)POM.[46] Standards determined not

308   to contribute significantly to the fit (value < 2σ) were removed, such that the only standards

309   included in the final LCA fits were $Tc(VII)O_4^-$, Tc(IV)-incorporated magnetite, which represents

310   Tc(IV) in an ordered iron oxide octahedral environment (as in goethite), and Tc(IV)EDTA,

311   which represents Tc(IV) in a disordered octahedral environment, e.g., surface sorbed, even

312   though EDTA is not present in the sample.

313   With an increase in $Fe(OH)_2(s)$, the amount of Tc(IV) incorporated into iron oxide

314   increases from 49(1)% (LAW-50-100Tc) to 63(1)% (LAW-200-100Tc). The remaining Tc(IV),

315   modeled as Tc(IV)EDTA, is presumably sorbed or loosely incorporated at the surface of the

316   solid where a disordered octahedral environment would be expected. Tc(IV) EDTA contributions

317   also remain relatively consistent between samples, 26(1)-30(1)%. Any remaining Tc is present as

318   $Tc(VII)O_4^-$ and decreases from 27.2(2)% to 9.0(3)% with increasing $Fe(OH)_2(s)$:simulant ratio.

319   The presence of Tc(VII) in LAW-200-100Tc is unsurprising considering a 200 g/L

320   Fe(OH)$_2$(s):simulant ratio is the requirement to remove 1 ppm of Tc(VII) from the simulant

321   (Figure 1), not 100 ppm of Tc(VII) as present in this sample.

322   When Tc speciation was analyzed for LAW-200-100Tc by XPS, the results were

323   significantly different from the bulk, with an almost equal distribution of Tc(VII) and Tc(IV)

324   (Table 2). This difference is likely due to facile reoxidation of surface adsorbed Tc(IV) relative

325   to Tc(IV) incorporated into the mineral. Such sensitivity to reoxidation is one difference between

326   Tc and Cr behavior in this system, since reduction of Cr(VI) produces stable, insoluble phases

327   including Cr(OH)$_3$ and Cr$_2$O$_3$ that do not require Cr incorporation into iron oxide/hydroxide

328   phases. Additionally, these results suggest that some surface specificity is provided by XPS,

329   despite the small goethite crystal size, or that goethite crystallites have agglomerated into larger

330   particles. It is important to note that Tc comprises only 0.14(3) atomic % of the LAW-200-100Tc

331   surface and was calculated while only considering Tc, Cr, Fe, O, and Cr constituents; therefore,

332   this contribution may be in fact lower.

333   *Local Coordination Environment of Tc in the Solid:* To evaluate how Tc(IV) is immobilized in

334   the solid, the local coordination environment of Tc in samples LAW-50-100Tc and LAW-200-

335   100Tc was determined using EXAFS. Goethite[39, 47] and magnetite[25] models, modified to account

336   for Tc substitution for Fe(III), were initially used to fit the EXAFS spectra. Difficulties

337   distinguishing between iron oxide/hydroxide environments is not uncommon, especially when

338   Tc(IV) is divided among several species.[6, 27, 48-49] In addition, the local environment of Fe(III) in

339   goethite is similar to that of the octahedral site of magnetite. In goethite, there are 4 Fe neighbors

340   at 3.1 Å and an additional 4 Fe neighbors at 3.6 A while in magnetite, there are 6 Fe neighbors at

341   3.0 Å and 6 at 3.5 Å. EXAFS analysis can determine distances more precisely (0.02 Å error)

342   than coordination numbers (20% error). For each sample, the R-factor determined using the

343 magnetite model was comparable if not better than the R-factor determined using the goethite

344 model. Furthermore, F-test results for evaluating the probability that an included scattering shell

345 contributes significantly to the EXAFS fit (SI Table S5) also favored the magnetite model.

346 However, given the increase in Tc-Fe bond lengths determined during fitting, which more

347 closely match the Fe-Fe bond lengths in goethite rather than magnetite, and the results from

348 XRD and XPS analyses, it is unlikely that magnetite is present in the solid phase. Therefore, Tc-

349 substituted goethite is assumed to be the most representative model and accounts for 30(8)% and

350 33(6)% of Tc in samples LAW-50-100Tc and LAW-200-100Tc, respectively (Table 3). This

351 distribution is lower than the range determined by XANES LCA, 49-63%, where a Tc-

352 incorporated magnetite standard is used to account for the ordered structural environment of the

353 iron (oxy)hydroxide phase rather than a goethite standard or model as used in the EXAFS

354 interpretation.

355   In addition to goethite, including $TcO_2 \cdot 2H_2O$ into the sample fits was required to account

356 for the portion of Tc(IV) sorbed or partially incorporated at the goethite surface. Tc(IV) sorbed

357 as $TcO_2 \cdot 2H_2O$ requires incorporation of a Tc–Tc neighbor (bond length ~2.57 Å) and a long Tc–

358 O bond (~2.47 Å) that accounts for the hydrated oxygen.[24] Although, in instances where Tc may

359 be partially incorporated into goethite, accounting for the long Tc – O bond often does not

360 significantly contribute to the EXAFS fit.[18] With this modification to the EXAFS fit, 67(6) % of

361 Tc was found to be present as sorbed or partially incorporated Tc(IV) in LAW-200-100Tc with

362 the hydrated Tc-O scatter pathway contributing significantly to the fit as indicated by a p value

363 (0.019) less than 0.05. For LAW-50-100Tc, including the long Tc–O bond did not significantly

364 contribute to the fit, thus suggesting partial incorporation of Tc(IV) into the solid phase of up to

365 42(7) %. This expansion to the sample EXAFS models aligns with interpretation of the XANES

366   spectra, which indicated that ≥26% of Tc(IV) is not completely incorporated into the iron

367   oxide/hydroxide solid.

368   Finally, for LAW-50-100Tc, where the $Fe(OH)_2(s)$:simulant ratio is too low to reduce

369   and immobilize all of the Tc present in solution, TcO_4^- was also included in the EXAFS fit and

370   accounted for 28(3)% of bulk Tc in the solid. TcO_4^- may persist as a dissolved species in

371   moisture retained by the sample between packaging and analysis or, if dried, as a pertechnetate

372   salt, e.g. $NaTcO_4$. Despite XANES indication LAW-200-100Tc contains 9% Tc(VII),

373   incorporating Tc(VII) into the EXAFS fit did not significantly improve the fit. The collected

374   EXAFS spectra, their Fourier transforms, and final fits are shown in Figure 3.
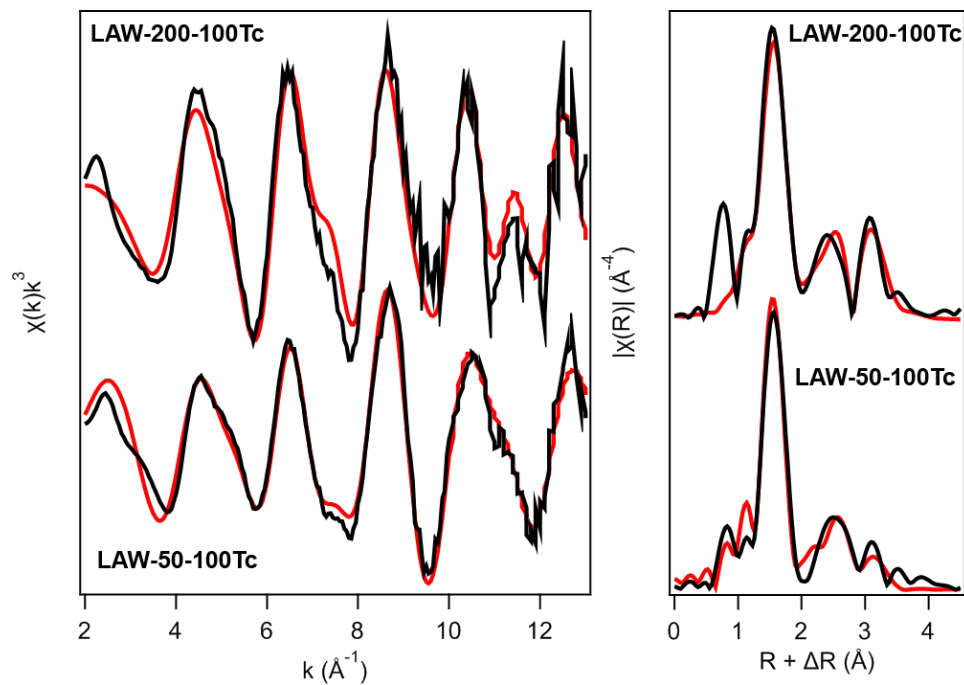
375

376   **Figure 3.** EXAFS spectra (left) and their Fourier transforms (right) for Tc-containing samples
377   LAW-200-100Tc (200 g/L $Fe(OH)_2(s)$:simulant ratio, 100 ppm Tc(VII)) and LAW-50-100Tc
378   (50 g/L $Fe(OH)_2(s)$:simulant ratio, 100 ppm Tc(VII). EXAFS fits (red) are based on a
379   combination of Tc-incorporated goethite, $TcO_2 \cdot 2H_2O$, and TcO_4^- (LAW-50-100Tc only) models.

380   **4. Environmental Implications**

381 One implication asserted after the first demonstration of Tc reduction and removal in the

382 presence of Cr by $Fe(OH)_2(s)$, was that $Fe(OH)_2(s)$ could be introduced into Hanford LAW to

383 form Tc-incorporated magnetite, which would stabilize Tc, decrease its volatility during

384 vitrification, and increase Tc loading in glass waste forms.[18] However, laboratory simulations of

385 $Fe(OH)_2(s)$ addition to LAW indicate that the amount of $Fe(OH)_2(s)$ required to remove Tc and

386 Cr is approximately one order of magnitude larger than the control system. Such a large increase

387 in $Fe(OH)_2(s)$ required to address Cr and Tc in LAW may adversely affect the final glass waste

388 form. Furthermore, under vitrification temperatures the stability of Tc is more favorable when

389 incorporated into the iron (oxy)hydroxide phase compared to $TcO_2 \cdot 2H_2O$.[6] As such, this system

390 would benefit from near complete incorporation of Tc into the goethite phase, which may require

391 additional $Fe(OH)_2(s)$ (>200 g/L). To this end $Fe(OH)_2(s)$ may be more appropriately used as a

392 localized remediation strategy for environmental contamination or for treating the less redox-

393 sensitive melter off-gas and secondary waste streams where the concentrations of Cr(VI), NO_2^-,

394 and other anions do not overwhelm the concentration of Tc(VII) by orders of magnitude.

395 **5. Supporting Information**

396 Additional analysis procedures and results for IC/ICP-MS, XPS, and EXAFS are provided in the

397 supporting information via the Internet at http://pubs.acs.org.

414

7. References

416 1.   Darab, J. G.; Smith, P. A., Chemistry of technetium and rhenium species during low-level
417 radioactive waste vitrification. *Chemistry of Materials* **1996,** *8* (5), 1004-1021.
418 2.   Luksic, S. A.; Riley, B. J.; Schweiger, M.; Hrma, P., Incorporating technetium in
419 minerals and other solids: A review. *Journal of Nuclear Materials* **2015,** *466*, 526-538.
420 3.   Banerjee, D.; Kim, D.; Schweiger, M. J.; Kruger, A. A.; Thallapally, P. K., Removal of
421 TcO4(-) ions from solution: materials and future outlook. *Chemical Society reviews* **2016,** *45*
422 (10), 2724-39.
423 4.   Zachara, J. M.; Ainsworth, C. C.; Brown, G. E.; Catalano, J. G.; McKinley, J. P.; Qafoku,
424 O.; Smith, S. C.; Szecsody, J. E.; Traina, S. J.; Warner, J. A., Chromium speciation and mobility
425 in a high level nuclear waste vadose zone plume. *Geochimica et Cosmochimica Acta* **2004,** *68*
426 (1), 13-30.
427 5.   Qafoku, O.; Pearce, C. I.; Neumann, A.; Kovarik, L.; Zhu, M.; Ilton, E. S.; Bowden, M.
428 E.; Resch, C. T.; Arey, B. W.; Arenholz, E.; Felmy, A. R.; Rosso, K. M., Tc(VII) and Cr(VI)
429 Interaction with Naturally Reduced Ferruginous Smectite from a Redox Transition Zone.
430 *Environmental Science & Technology* **2017,** *51* (16), 9042-9052.
431 6.   Um, W.; Luksic, S. A.; Wang, G.; Saslow, S.; Kim, D.-S.; Schweiger, M. J.; Soderquist,
432 C. Z.; Bowden, M. E.; Lukens, W. W.; Kruger, A. A., Enhanced 99Tc retention in glass waste
433 form using Tc(IV)-incorporated Fe minerals. *Journal of Nuclear Materials* **2017,** *495*
434 (Supplement C), 455-462.
435 7.   Kim, D.; Kruger, A. A., Volatile species of technetium and rhenium during waste
436 vitrification. *Journal of Non-Crystalline Solids* **2018,** *481* (Supplement C), 41-50.
437 8.   Lee, M.-S.; Um, W.; Wang, G.; Kruger, A. A.; Lukens, W. W.; Rousseau, R.; Glezakou,
438 V.-A., Impeding [99]Tc(IV) mobility in novel waste forms. *Nature Communications* **2016,** *7*.

439   9.   Smith, F. N.; Um, W.; Taylor, C. D.; Kim, D. S.; Schweiger, M. J.; Kruger, A. A.,
440   Computational Investigation of Technetium(IV) Incorporation into Inverse Spinels: Magnetite
441   (Fe3O4) and Trevorite (NiFe2O4). *Environ Sci Technol* **2016,** *50* (10), 5216-24.
442   10.   Smith, F. N.; Taylor, C. D.; Um, W.; Kruger, A. A., Technetium Incorporation into
443   Goethite (alpha-FeOOH): An Atomic-Scale Investigation. *Environ Sci Technol* **2015,** *49* (22),
444   13699-707.
445   11.   Skomurski, F. N.; Rosso, K. M.; Krupka, K. M.; McGrail, B. P., Technetium
446   Incorporation into Hematite (α-Fe$_2$O$_3$). *Environmental Science & Technology* **2010,** *44* (15),
447   5855-5861.
448   12.   Lukens, W. W.; Magnani, N.; Tyliszczak, T.; Pearce, C. I.; Shuh, D. K., Incorporation of
449   technetium into spinel ferrites. *Environmental Science & Technology* **2016,** *50* (23), 13160-
450   13168.
451   13.   Lukens, W. W.; Saslow, S. A., Aqueous Synthesis of Technetium-Doped Titanium
452   Dioxide by Direct Oxidation of Titanium Powder, a Precursor for Ceramic Nuclear Waste
453   Forms. *Chemistry of Materials* **2017,** *29* (24), 10369-10376.
454   14.   Pepper, S. E.; Bunker, D. J.; Bryan, N. D.; Livens, F. R.; Charnock, J. M.; Pattrick, R. A.
455   D.; Collison, D., Treatment of radioactive wastes: An X-ray absorption spectroscopy study of the
456   reaction of technetium with green rust. *Journal of Colloid and Interface Science* **2003,** *268* (2),
457   408-412.
458   15.   Zhdanov, S., Encyclopedia of the electrochemistry of the elements. *by AJ Bard, Marcel*
459   *Dekker, New York* **1975,** *4*, 362.
460   16.   Rard, J. A.; Rand, M.; Anderegg, G.; Wanner, H., *Chemical thermodynamics of*
461   *technetium*. Elsevier Publishing Company: 1999.
462   17.   Russell, R. L.; Westsik Jr, J.; Swanberg, D. J.; Eibling, R. E.; Cozzi, A.; Lindberg, M. J.;
463   Josephson, G. B.; Rinehart, D. E. *Letter report: LAW simulant development for cast stone*
464   *screening tests*; Pacific Northwest National Laboratory: Richland, WA, 2013.
465   18.   Saslow, S. A.; Um, W.; Pearce, C. I.; Engelhard, M. H.; Bowden, M. E.; Lukens, W.;
466   Leavy, II; Riley, B. J.; Kim, D. S.; Schweiger, M. J.; Kruger, A. A., Reduction and Simultaneous
467   Removal of 99Tc and Cr by Fe(OH)2(s) Mineral Transformation. *Environ Sci Technol* **2017,** *51*
468   (15), 8635-8642.
469   19.   Gephart, R. E.; Lundgren, R. E. *Hanford tank clean up: A guide to understanding the*
470   *technical issues*; PNL-10773; Pacific Northwest National Laboratory: Richland, WA., 1995; p
471   80.
472   20.   Certa, P.; Empey, P.; Wells, M., River Protection Project System Plan ORP-11242
473   Revision 6. *Washington River Protection Solutions, LLC, Richland, Washington* **2011**.
474   21.   Oostrom, M.; Truex, M. J.; Last, G. V.; Strickland, C. E.; Tartakovsky, G. D., Evaluation
475   of deep vadose zone contaminant flux into groundwater: Approach and case study. *Journal of*
476   *Contaminant Hydrology* **2016,** *189*, 27-43.
477   22.   Webb, S. M., SIXpack: a graphical user interface for XAS analysis using IFEFFIT.
478   *Physica Scripta* **2005,** *2005* (T115), 1011.
479   23.   Ravel, B.; Newville, M., ATHENA, ARTEMIS, HEPHAESTUS: Data analysis for X-ray
480   absorption spectroscopy using IFEFFIT. *Journal of Synchrotron Radiation* **2005,** *12* (4), 537-
481   541.
482   24.   Lukens, W. W.; Bucher, J. J.; Edelstein, N. M.; Shuh, D. K., Products of pertechnetate
483   radiolysis in highly alkaline solution: Structure of TcO$_2 \cdot x$H$_2$O. *Environmental Science &*
484   *Technology* **2002,** *36* (5), 1124-1129.

485   25.   Wechsler, B. A.; Lindsley, D. H.; Prewitt, C. T., Crystal structure and cation distribution
486   in titanomagnetites ($Fe_{3-x}Ti_xO_4$). *American Mineralogist* **1984,** *69* (7-8), 754-770.
487   26.   Marshall, T. A.; Morris, K.; Law, G. T. W.; Mosselmans, J. F. W.; Bots, P.; Parry, S. A.;
488   Shaw, S., Incorporation and retention of 99-Tc(IV) in magnetite under high pH conditions.
489   *Environmental Science & Technology* **2014,** *48* (20), 11853-11862.
490   27.   Um, W.; Chang, H.-S.; Icenhower, J. P.; Lukens, W. W.; Serne, R. J.; Qafoku, N. P.;
491   Westsik, J. H.; Buck, E. C.; Smith, S. C., Immobilization of 99-technetium (VII) by Fe(II)-
492   goethite and limited reoxidation. *Environmental Science & Technology* **2011,** *45* (11), 4904-
493   4913.
494   28.   Kendelewicz, T.; Liu, P.; Doyle, C. S.; Brown Jr, G. E., Spectroscopic study of the
495   reaction of aqueous Cr(VI) with Fe_3O_4 (111) surfaces. *Surface Science* **2000,** *469* (2–3), 144-
496   163.
497   29.   Kendelewicz, T.; Liu, P.; Doyle, C. S.; Brown Jr, G. E.; Nelson, E. J.; Chambers, S. A.,
498   X-ray absorption and photoemission study of the adsorption of aqueous Cr(VI) on single crystal
499   hematite and magnetite surfaces. *Surface Science* **1999,** *424* (2–3), 219-231.
500   30.   Fanning, J. C., The chemical reduction of nitrate in aqueous solution. *Coordination*
501   *Chemistry Reviews* **2000,** *199* (1), 159-179.
502   31.   Brylev, O.; Sarrazin, M.; Roué, L.; Bélanger, D., Nitrate and nitrite electrocatalytic
503   reduction on Rh-modified pyrolytic graphite electrodes. *Electrochimica Acta* **2007,** *52* (21),
504   6237-6247.
505   32.   Zachara, J. M.; Heald, S. M.; Jeon, B.-H.; Kukkadapu, R. K.; Liu, C.; McKinley, J. P.;
506   Dohnalkova, A. C.; Moore, D. A., Reduction of pertechnetate [Tc(VII)] by aqueous Fe(II) and
507   the nature of solid phase redox products. *Geochimica et Cosmochimica Acta* **2007,** *71* (9), 2137-
508   2157.
509   33.   Wells, M.; Fitzpatrick, R. W.; Gilkes, R., Thermal and mineral properties of Al-, Cr-,
510   Mn-, Ni-and Ti-substituted goethite. *Clays and Clay Minerals* **2006,** *54* (2), 176-194.
511   34.   Schikorr, G., Über die Reaktionen zwischen Eisen, seinen Hydroxyden und Wasser.
512   *Zeitschrift für Elektrochemie und angewandte physikalische Chemie* **1929,** *35* (2), 65-70.
513   35.   He, Y. T.; Traina, S. J., Cr(VI) Reduction and Immobilization by Magnetite under
514   Alkaline pH Conditions: The Role of Passivation. *Environmental Science & Technology* **2005,**
515   *39* (12), 4499-4504.
516   36.   Jolivet, J.-P.; Chanéac, C.; Tronc, E., Iron oxide chemistry. From molecular clusters to
517   extended solid networks. *Chemical Communications* **2004,** (5), 481-483.
518   37.   Um, W.; Chang, H.; Icenhower, J. P.; Lukens, W. W.; Jeffrey Serne, R.; Qafoku, N.;
519   Kukkadapu, R. K.; Westsik, J. H., Iron oxide waste form for stabilizing 99Tc. *Journal of Nuclear*
520   *Materials* **2012,** *429* (1-3), 201-209.
521   38.   Shannon, R., Revised effective ionic radii and systematic studies of interatomic distances
522   in halides and chalcogenides. *Acta Crystallographica Section A* **1976,** *32* (5), 751-767.
523   39.   Schwertmann, U.; Gasser, U.; Sticher, H., Chromium-for-iron substitution in synthetic
524   goethites. *Geochimica et Cosmochimica Acta* **1989,** *53* (6), 1293-1297.
525   40.   Shannon, R. D.; Prewitt, C. T., Effective ionic radii in oxides and fluorides. *Acta*
526   *Crystallographica Section B* **1969,** *25* (5), 925-946.
527   41.   Fazey, P.; O'Connor, B.; Hammond, L., X-ray powder diffraction Rietveld
528   characterization of synthetic aluminum-substituted goethite. *Clays and Clay Minerals* **1991,** *39*
529   (3), 248-253.

530   42.   Alvarez, M.; Rueda, E. H.; Sileo, E. E., Simultaneous incorporation of Mn and Al in the
531   goethite structure. *Geochimica et Cosmochimica Acta* **2007,** *71* (4), 1009-1020.
532   43.   Farges, F., Chromium speciation in oxide-type compounds: application to minerals,
533   gems, aqueous solutions and silicate glasses. *Phys Chem Minerals* **2009,** *36* (8), 463-481.
534   44.   Nyburg, S. C.; Steed, J. W.; Aleksovska, S.; Petrusevski, V. M., Structure of the alums. I.
535   On the sulfate group disorder in the [alpha]-alums. *Acta Crystallographica Section B* **2000,** *56*
536   (2), 204-209.
537   45.   Giovanoli, R.; Stadelmann, W.; Feitknecht, W., Über kristallines Chrom (III) hydroxid. I.
538   *Helvetica Chimica Acta* **1973,** *56* (3), 839-847.
539   46.   McGregor, D.; Burton-Pye, B. P.; Howell, R. C.; Mbomekalle, I. M.; Lukens, W. W.;
540   Bian, F.; Mausolf, E.; Poineau, F.; Czerwinski, K. R.; Francesconi, L. C., Synthesis, Structure
541   Elucidation, and Redox Properties of 99Tc Complexes of Lacunary Wells−Dawson
542   Polyoxometalates: Insights into Molecular 99Tc−Metal Oxide Interactions. *Inorganic Chemistry*
543   **2011,** *50* (5), 1670-1681.
544   47.   Szytuła, A.; Burewicz, A.; Dimitrijević, Ž.; Kraśnicki, S.; Rżany, H.; Todorović, J.;
545   Wanic, A.; Wolski, W., Neutron Diffraction Studies of α-FeOOH. *physica status solidi (b)* **1968,**
546   *26* (2), 429-434.
547   48.   Peretyazhko, T.; Zachara, J. M.; Heald, S. M.; Jeon, B. H.; Kukkadapu, R. K.; Liu, C.;
548   Moore, D.; Resch, C. T., Heterogeneous reduction of Tc(VII) by Fe(II) at the solid–water
549   interface. *Geochimica et Cosmochimica Acta* **2008,** *72* (6), 1521-1539.
550   49.   Masters-Waage, N. K.; Morris, K.; Lloyd, J. R.; Shaw, S.; Mosselmans, J. F. W.;
551   Boothman, C.; Bots, P.; Rizoulis, A.; Livens, F. R.; Law, G. T. W., Impacts of Repeated Redox
552   Cycling on Technetium Mobility in the Environment. *Environmental Science & Technology*
553   **2017,** *51* (24), 14301-14310.

554

555

556 Tables.

557 **Table 1.** 5 M Na Average LAW Simulant Composition

Constituent	Target Concentration [mg/L]*	Concentration [mg/L]	Constituent	Target Concentration [mg/L]*	Concentration [mg/L]
Al	8280	8500	F-	600	<1000
Cr	1120	1080	Cl-	1500	<2500
P	1520	981	NO_2^-	26,000	26,800
K	1280	1300	Br-	-	<5000
Na	115,000	110,000	NO_3^-	101,000	102,000
S	2740	2810	SO_4^-	-	10,100
Ti	-	7.84	PO_4^-	-	<7500
pH		13.5			

* Target Concentrations from Russell et al, 2013.[17]
-: Not identified

558

559 **Table 2.** XRD and High Resolution XPS Analysis of Select Solid Phases

Sample		LAW-50-0Tc-1	LAW-100-0Tc	LAW-200-100Tc
$Fe(OH)_2(s)$:Simulant Ratio	*g/L*	50	100	200
Starting [Tc(VII)]	*ppm*	0	0	100
XRD Analysis				
Goethite (α-FeOOH)	*wt%*	77	81	-
a	*(Å)**	4.602(2)	4.597(3)	-
b	*(Å)**	9.920(3)	9.913(2)	-
c	*(Å)**	3.0096(9)	3.0080(9)	-
Crystal Size	*(nm)***	9.8(1)	10.7(1)	-
Feroxyhyte (δ-FeOOH)	*wt%*	17	14	-
Hematite (Fe_2O_3)	*wt%*	-	3	-
Amorphous/Unidentified	*wt%*	6	1	-
*Survey XPS Analysis***				
Cr 2p	*at %**	1.6(1)	1.1(1)	0.13(1)
Tc 3d	*at %*	-	-	0.14(3)
Fe 2p	*at %*	7.3(4)	8.4(8)	1.7(2)
C 1s	*at %*	27(4)	19(6)	24(1)
O 1s	*at %*	64(3)	71(5)	74(1)
*Cr XPS Analysis***				
CrOOH	*at %*	46(1)	38(14)	59(2)
Cr_2O_3	*at %*	28(10)	43(19)	32(4)
$Cr(OH)_3$	*at %*	24.7(2)	18(5)	1(2)
Cr(VI)	*at %*	1.5	1.3(5)	8.3(8)
*Tc XPS Analysis***				
Tc(VII)	*at %*	-	-	52(1)
Tc(IV)	*at %*	-	-	48(1)
*Fe XPS Analysis***				
$FeCr_2O_4$	*at %*	0	0	5.7(2)
Fe_3O_4	*at %*	12(1)	11(2)	11(1)
FeOOH	*at %*	88(1)	89(2)	83(1)

(-) No Detected or Analyzed (*) Atomic percent
Goethite (α-FeOOH)[33]: a = 4.634 Å, b = 9.945 Å, c = 3.0321 Å
*Values in parentheses are ±3σ, based on the error associated with the Reitveld refinement.
** Values in parentheses are ±1σ. For XPS, the standard deviation is determined from of the average of two replicate spot analyses collected for each sample.

560

561 **Table 3.** LCA and EXAFS Results from Cr and Tc K Edge XANES and EXAFS Spectra

Sample		LAW-50-0Tc	LAW-50-100Tc	LAW-200-100Tc
$Fe(OH)_2(s)$:Simulant Ratio	g/L	50	50	200
Starting [Tc(VII)]	ppm	0	100	100
Cr XANES LCA Analysis				
Cr Alum ($KCr(SO_4)_2 \cdot 12H_2O$)	%	35(1)	35(1)	38(4)
	p*	<0.001	<0.001	<0.001
$Fe_{2.5}Cr_{0.5}O_4$	%	58(2)	59(2)	62(4)
	p	<0.001	<0.001	<0.001
$FeCr_2O_4$	%	6(1)	6(1)	-
	p	0.287	0.304	-
Tc XANES LCA Analysis				
TcO_4^-	%	-	27.2(2)	9.0(3)
	p	-	<0.001	<0.001
Tc(IV) Incorporated Fe_3O_4	%	-	49(1)	63(1)
	p	-	<0.001	<0.001
Tc(IV) EDTA	%	-	26(1)	30(1)
	p	-	<0.001	<0.001
Tc EXAFS Analysis				
TcO_4^-	%	-	33(6)	0(0)
$TcO_2 \cdot 2H_2O$	%	-	32(8)	67(6)
Goethite	%	-	35(3)	33(6)

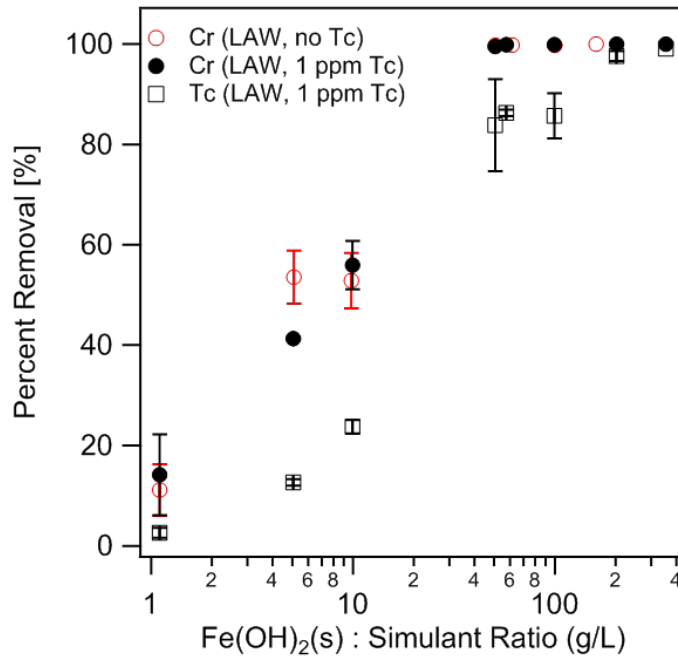Values in parenthesis indicate the standard deviation of the last significant figure.
(-) No Detected
(*) Probability that the improvement to the fit by adding the scattering shell is due to random error. A p value < 0.05 indicates that the improvement is greater than 2σ of the fit.

562
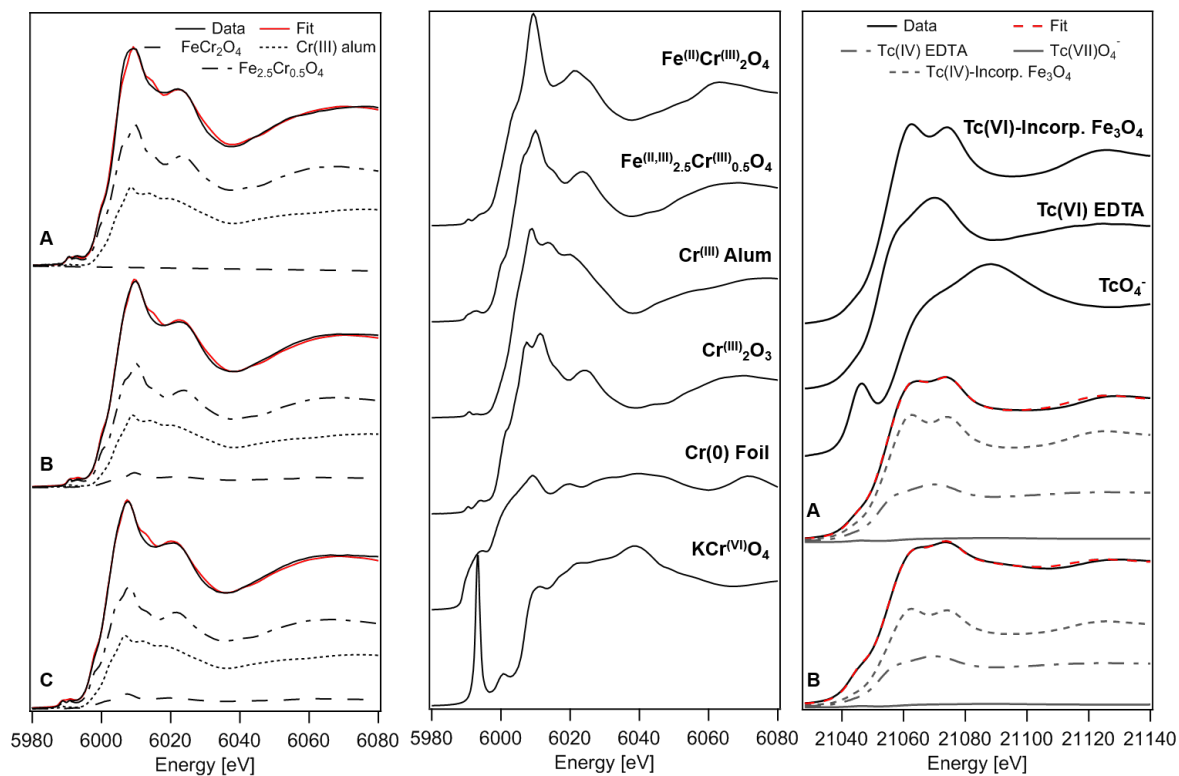
563

564 Figures.

565

566

567 **Figure 1.** Cr and Tc removal from LAW simulant with 1 ppm Tc (black) and without Tc (red).
568 Cr(VI) results are indicated by filled circles, Tc results by open squares. Error bars represent the
569 standard deviation of results averaged from two to six replicate samples. Percent removal
570 assumed to be 100% if below ICP-OES detection limit for Cr (23 µg/L) or ICP-MS detection
571 limit for Tc (33 ng/L).

572

573

574

Figure 2. (Left) Normalized and off-set Cr K edge XANES spectra with corresponding LCA fits for Fe(OH)$_2$(s):Simulant ratios (A) 200 g/L, 100 ppm Tc(VII), (B) 50 g/L, 100 ppm Tc(VII), and (C) 50 g/L, no Tc(VII). The LCA fit (red) to the data (black) is the sum of the standard contributions from FeCr$_2$O$_4$ (dash line), Fe$_{2.5}$Cr$_{0.5}$O$_4$ (dot/dash line), and Cr alum (dotted line) determined in the final fit. (Middle) Cr standards considered during LCA fitting, off-set for clarity. (Right) Normalized and off-set Tc K-edge XANES spectra (black) for samples A and B from left panel and the final Tc standards used during LCA fitting. The Tc LCA fit (red dashed line) is the sum of the standard contributions from TcO$_4^-$ (line), TcEDTA (dot/dash), and Tc-incorporated Fe$_3$O$_4$ (dash).

584

585

586
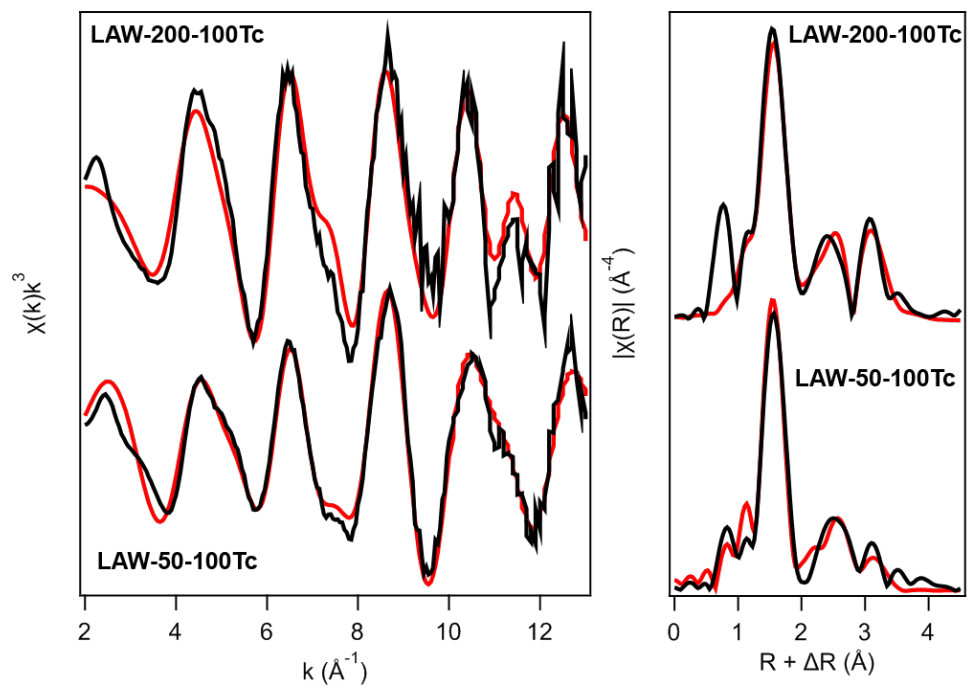
587

588

589

590

591

592

Figure 3. EXAFS spectra (left) and their Fourier transforms (right) for Tc-containing samples LAW-200-100Tc and LAW-50-100Tc. EXAFS fits (red) are based on a combination of Tc-incorporated goethite, $TcO_2 \cdot 2H_2O$, and TcO_4^- (LAW-50-100Tc only) models.

596